SUITABILITY OF THE SHARP JX-600 DESKTOP SCANNER FOR THE DIGITIZATION OF AERIAL COLOR PHOTOGRAPHS

Tapani Sarjakoski
Finnish Geodetic Institute
Ilmalankatu 1 A
SF-00240 Helsinki
Finland

Commission II

ABSTRACT

Digitization of aerial photographs is one of the bottlenecks in the current transition phase in the introduction of fully digital photogrammetric systems. Owing to their low cost, desktop scanners offer an interesting alternative. This paper examines as a case study the suitability of the Sharp JX-600 desktop scanner for the digitization of aerial color photographs. The structure of the scanner is reviewed. A method for calibrating the scanner geometrically is given and the calibration results are presented. The image quality of the scanned images is analyzed. Finally, a method is introduced for calibrating the scanner individually for each scanned image.

KEYWORDS: Image scanner, Digital color images, Calibration, Geometry

1. INTRODUCTION

We are currently going over from analog/analytical photogrammetric methods to fully digital/analytical methods. Computer technology is now mature enough to handle large digital imageries related to aerial photographs. There are available powerful personal computers or workstations that are well suited for interactive work with large digital imageries when furnished with appropriate photogrammetric/mapping/GIS software. Mass-storage devices, such as conventional magnetic disks, opto-magnetic disk-drives and DAT tape-drives, offer adequate storage capacity for aerial images, especially if the medium resolution (50μm - 30μm pixel size) is used.

However, the transition phase is not going as smoothly as it might owing to certain bottlenecks; one of these is digitization of aerial photographs by scanning. High-precision scanners suitable for photogrammetric work certainly exist, but their price is so high that they are beyond the pocket of many potential users of digital photogrammetric methods.

Owing to their low cost, desktop scanners offer an interesting alternative for digitization. They have been designed mainly for use in color publishing tasks. A typical desktop scanner has a scanning area of A4 or A3 size and a spatial resolution of up to 600 dpi. Spectral resolution typically varies from 8-bit grayscale to 24-bit RGB color.

This paper evaluates the suitability of the Sharp JX-600 desktop scanner for the digitization of aerial color photographs. Some other scanners have similar specifications and thus the methods and recommendations discussed here may also have more general applicability. The emphasis is on the geometric aspects of the scanner. It is in our interest to establish if the inherent "weaknesses" of the scanner could be taken into account so that scanned images could be used for photogrammetric purposes. A calibration procedure and a subsequent digital rectification process for the scanned images are seen as a way of producing distortion-free output images.

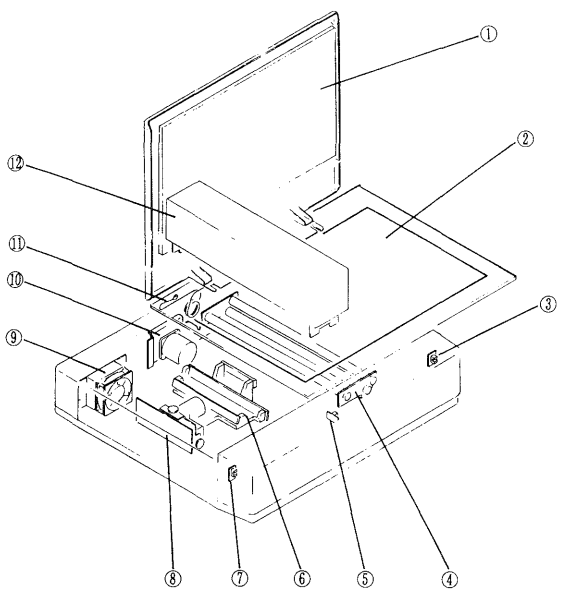

Fig. 7-1

① OR (Original) cover unit
② Table glass
③ WB (White balance) sensor
④ Fluorescent lamp unit
⑤ Lamp unit sensor
⑥ Optical system unit
⑦ Left sensor
⑧ CCD board (in the optical system unit)
⑨ Fan
⑩ Drive unit
⑪ Table drive wire
⑫ Lamp unit

Figure 1. The general structure of Sharp JX-600[1].

[1]Figures 1, 2, and 3 have been quoted from Sharp JX-600 Service Manual, with the permission of Sharp Electronics (Europe) GMBH.

2. OPTO-MECHANICAL STRUCTURE OF THE SHARP JX-600 DESKTOP SCANNER

2.1 General Description

The Sharp JX-600 is a so-called flatbed scanner. The original document is held in a moving glass-plate table. The whole image is digitized by a line sequential scanning in which the table - driven by a stepping motor - is moved (Figure 1). The intensity values within a line are recorded by a MN3666 CCD linear image sensor, which has 7500 photoelectronic conversion elements of 6 µm arranged in a straight line in a 9 µm pitch. Light is transmitted from the table to the CCD sensor with an optical system consisting of a lens and three mirrors (Figure 2). The reduction factor is 4.7 so that the 9 µm pitch equals 42.3 µm on the plate. The largest image size is 10200 x 7032 elements with 600 dpi resolution. Color images are scanned in one pass, and colors are separated with a flashing three-color fluorescent lamp unit. A separate lamp unit is placed above the table for scanning transparent originals.

2.2 The Geometrical Quality of Images

Two aspects of the geometrical quality of digital output images deserve special attention: 1) permanent geometrical distortions and 2) repeatability in the geometrical sense. Given the characteristics of the SHARP JX-600 scanner, what kind of geometrical quality can we expect? The following characteristics of the opto-mechanical structure of the scanner are important:

- CCD-sensor. This construction uses a single linear CCD array. Taking this into account and also the type of device (solid-state), the geometrical quality of a single scanned line is not likely to be deteriorated.
- Optical System. The optical system can be divided into two parts: 1) the body of the scanner and 2) the moving table.

The body of the scanner consists of the CCD sensor, a reduction lens and three mirrors, all mounted in a rather robust frame. The position of the lens and the CCD array can be adjusted with alignment screws. It can be assumed that the system is stable. The most suspectable element of the system is the reduction lens, its geometrical distortions will directly affect the geometry of the output image. Moreover, radial distortion would affect the main-scan direction, and tangential distortion would cause the image to be bent or curved in the same direction. Such effects are even likely because of the rather simple lens used. Any bends in the mirrors would cause similar effects. Improper angular alignment of the optical system with respect to the body and the table of the scanner would result non-orthogonality to the output image.

The glass plate - part of the moving table - will affect the geometry of the image. However, the thickness of the glass plate is not likely to vary so much that it would cause problems (See also 2.2.3, Flatness of the Table).

2.2.1 Guides of the Table. The moving table has an asymmetric guide system. On the drive- (rear) side there is a double-U guide with ball bearings that controls the table vertically and horizontally. On the opposite side (front) of the table there is no horizontal guidance; the vertical guidance is realized so that the glass plate of the table lies directly on a hard-plastic coated track. This solution does not prevent the table from being lifted from the track if any force is applied in this direction. Thus the following image geometry-related features are typical for this construction:

- Any bends in the two double-U guides would cause corresponding regular deformations in the image.
- Any slackness in the bearings of the double-U guides would cause irregular deformations in the image.
- Any lift in the front side of the table will affect the image, owing to the "free guidance" of the front side.
- The asymmetry of the guide-system and the "free guidance" of the front side may be favorable, as tensions in the drive system will be avoided.

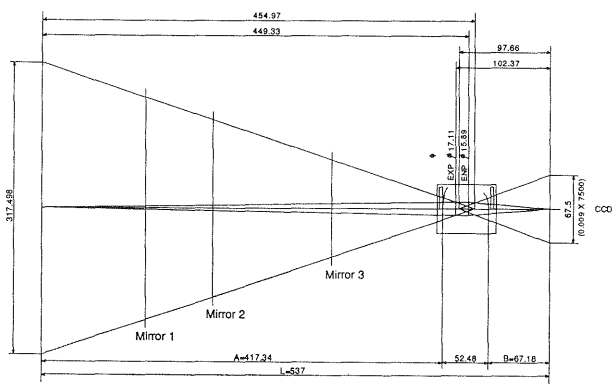

Figure 2. The optical system of Sharp JX-600.

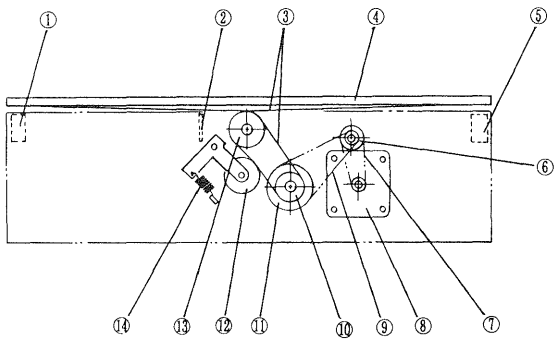

Fig. 7-3

① WB sensor
② Lamp unit sensor
③ Table drive wire
④ Table glass
⑤ Left sensor
⑥ Reduction pulley
⑦ Belt 1
⑧ Pulse motor (About 0.02116mm/step)
⑨ Belt 2
⑩ Drive pulley
⑪ Idle pulley
⑫ Tension pulley
⑬ Wire pulley
⑭ Tension spring

Figure 3. The drive system of Sharp JX-600.

Note that any vertical translocation of the table or the original image will yield a translation in the main-scan direction. This effect is especially strong at the edges of the scanning area, where the direction of the optical beams is such that a 100 µm vertical shift corresponds to a shift of 35 µm in the main-scan direction.

2.2.2 Drive System of the Table. The drive system moves the table in the sub-scanning direction. The system is driven by a pulse motor, which drives the idle pulley via two belts. The idle pulley drives the wire around the drive pulley and moves the table back and forth (Figure 3). With respect to the geometry of the output image, there are some inherent weaknesses in the drive system. Any eccentricities in the pulleys will cause periodic errors in the sub-scan direction. Irregularities in the strength of the belts and the wire would probably cause similar effects. Such errors presumably remain stable from scan to scan within a short period of time. However, if any of the belts or wires slide on the pulley, the zero point of the corresponding periodic error is moved, and the probalbly regular pattern of systematic errors in the sub-scan direction would be different.

2.2.3 Flatness of the Table. If there are any irregular deformations in the flatness of the glass plate of the table, the corresponding errors would show up in the main-scan direction. Because of the direction of the optical beams, this effect would be at its minimum (zero) in the central axis of the table and at its maximum in both edges.

2.2.4 Flatness of the Document. In this context flatness of the document means the tightness of document to be scanned against the table. If the flatness is not sufficient, the effect would be exactly the same as with the lacking flatness of the table. The flatness is guaranteed rather well when a paper original is scanned because the cover unit presses the original firmly against the glass. When diapositives are scanned, a plastic scattering plate is placed on the top of the diapositive. This plate is very light and does not assure sufficient pressure to keep the diapositive flat.

2.2.5 Color Separation. Color images are scanned in one pass, and the colors are separated with a three-color fluorescent lamp unit. This approach seems to be very robust in that it guarantees the correct geometric registration between the three-color elements.

3. CALIBRATION

3.1 Error Model

Based on the reasoning above and some experimental calibration attempts, a functional error model comprising the following two polynomial-type parts was defined:

$$dy = a_1 y + a_2 y^2 \quad (1)$$

$$dx = b_1 x + b_2 y + b_3 y^2 + c_1 I_1 + \ldots + c_n I_n \quad (2)$$

y = pixel coordinate in the main-scan direction (column, direction of the CCD-sensor)

x = pixel coordinate in the sub-scan direction (line, movement of the table)

dx, dy = respective geometric deformations

a_1 = scale error in the main-scan direction

a_2 = error in the main-scan direction, due to the 2nd order radial distortion of the lens

b_1 = scale error in the sub-scan direction

b_2 = non-orthogonality of the image

b_3 = error in the sub-scan direction, due to the 2nd order tangential distortion of the lens

$c_1, \ldots, c_n$ = local errors in the sub-scan direction (this model approximates the local errors, which are assumed to be constant within a certain interval, 20 -200 lines, depending on the selection of n)

$I_1, \ldots, I_n$ = coefficients for the local errors ($I_i = 1$ if $y/n = i$, otherwise $I_i = 0$)

The general principle in the model is that the shape and size of any geometric feature on the original image should be retained on the digital output image. The polynomials dx and dy describe the deviations that may occur between the two images. The model includes first- and second-order terms for the errors caused by the optical system. The periodic errors in the sub-scan direction are modeled simply by assuming the error to be constant within a short interval. More sophisticated models (such as one based on piecewise linear interpolation) could be applied but this was not considered necessary in the present study.

3.2 Calibration Setup

The values of the error model were determined with a photogrammetric precision grid or gitter. The gitter has a grid of lines in an area of 230 x 230 mm^2, the interval between the lines being precisely 10 mm except for the 2 outermost lines for which the interval is 5 mm (Figure 4). The grid lines are engraved on a thick (about 10 mm) glass plate.

The gitter was scanned in four different positions so that the scanning area was covered rather completely. Each time the gitter was in a slightly tilted position (Figure 4). This assures that the whole area is covered with observations (see below). The image size was 10200 x 7032 pixels in each of the four scans. All four scans were completed within about 2 hours.

3.3 Determination of Line Deformations by Digital Methods

The next step in the calibration procedure was to determine the line deformations. This step was repeated for each of the four images separately. In this context line deformation means the displacement of the gitter lines with respect to their correct or ideal position. All the grid lines were divided into 46 sections 4.5 mm long, the line crossings being outside the sections. The displacement in perpendicular direction with respect to the line was determined for each section. These displacements were determined keeping an ideal grid (rectangular in correct scale) as a reference. The position of this reference was defined approximately by pointing four corner points of the grid and adjusting the grid to them with least-squares adjustment.

The objective of this phase was to determine the perpendicular displacements in sub-pixel accuracy. The displacement values were determined using digital image processing methods. With the approximate position of the ideal grid as a starting point, a 4.4 mm x 0.8 mm rectangle was defined around each line section. This rectangle was further divided into 68 bins (Figure 5). The pixels having the lowest gray-level values were located within each bin, and the average of their displacement values was used as a displacement value for the bin. Finally, the displacement value for the whole section was computed as the average of the bin displacement values.

The procedure described above was developed by trial and error. It proved to be rather robust with respect to the distribution or histogram of the graylevel values. As will be seen below, it certainly produces displacement values in sub-pixel accuracy. This is due partly to the method of multiple averaging but partly to the tilted position of the grids, which causes an aliasing effect on the lines. Some earlier experiments indicated clearly that accuracy will be degraded if the tilt is very small (less than 20 mm over the whole 230 mm edge).

3.4 Estimation of the Error Model

The parameters of the error model were estimated by least squares adjustment in which the displacement values were treated as observations. All four images were treated simultaneously using the following the adjustment model:

$$DX_{ji} = A_j - C_j Y_{ji} + \cos(a_j)\, dx(x_{ji}, y_{ji}) - \sin(a_j)\, dy(x_{ji}, y_{ji}) \quad (3)$$

$$DY_{ji} = B_j + C_j X_{ji} + \cos(a_j)\, dy(x_{ji}, y_{ji}) + \sin(a_j)\, dx(x_{ji}, y_{ji}) \quad (4)$$

j	=	index for each image
i	=	index for each line section or observation
X_{ji}, Y_{ji}	=	grid coordinates of the center point of line section (the axes of the XY-coordinate system coincide with the grid lines)
DX_{ji}	=	the displacement value for Y-axis directed line sections
DY_{ji}	=	the displacement value for X-axis directed line sections
A_j, B_j, C_j	=	the three parameters for free shift and rotation of the grid in each of the images (j)
x_{ji}, y_{ji}	=	image coordinates of the center point of a line section (ij)
$dx(x_{ji}, y_{ji})$	=	the total effect (in the sub-scan direction) of the error model for a line section (ij)
$dy(x_{ji}, y_{ji})$	=	the total effect (in the main-scan direction) of the error model for a line section (ij)
a_j	=	tilt angle of the grid in each of the images (j).

The parameters for free shift and rotation of the grid in each image are necessary because the position and rotation of the grid is known only approximately within each image. As the tilt angle is rather small, the values of cos(aj) and sin(aj) are close to 1 and 0, respectively. Therefore the errors in main- and sub-scan direction will mainly affect DY and DX, respectively. The adjustment model is based on the assumption that errors are repeatable, .i.e, there is no significance difference in the systematic errors between any two scans. The validity of this assumption is studied below.

The parameters of the adjustment model were solved by the least-squares adjustment using the displacement values of the line sections as observations or sample points.

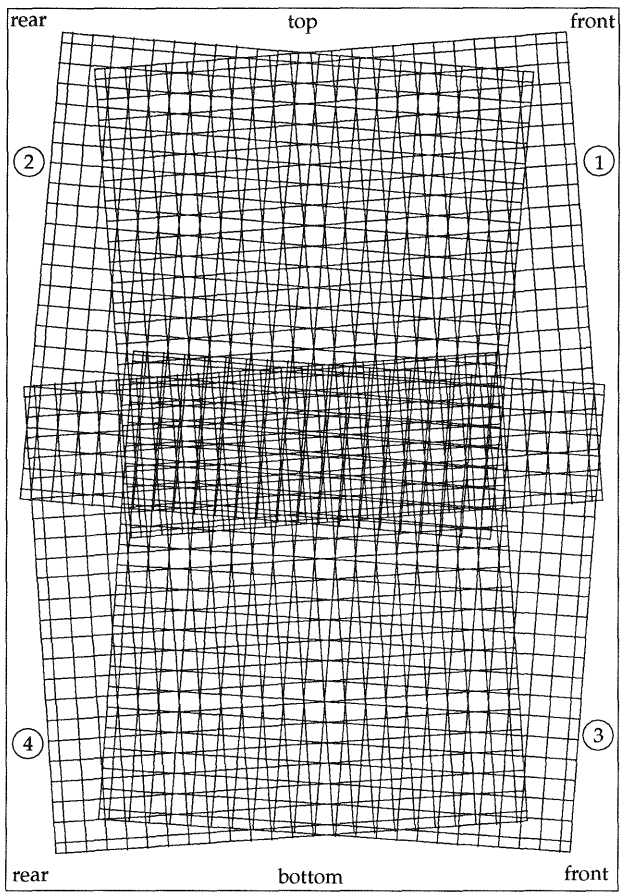

Figure 4. The grid pattern and the four set-ups of the precision gitter used in calibration.

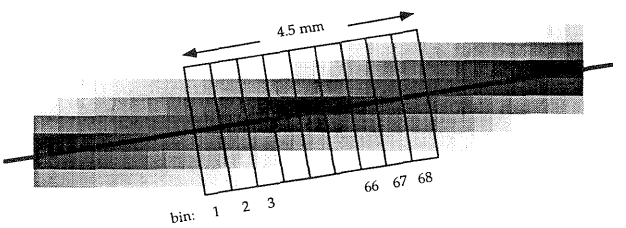

Figure 5. A graphical illustration of the method used to compute the displacement of a line section. The displacement value is computed as the average of the value of each bin. For each bin the displacement value is obtained as the average of the perpendicular distances of the centers of the "darkest" pixels, using the ideal position of the line (dark line) as a reference.

3.5 Summary of the Calibration Results

The main results of the calibration are given in Tables 1-2 and Figures 6-12.

Preliminary adjustments showed that the polynomial terms a_1 , a_2 , b_1 , b_2 , b_3 get significant values in conjunction with any data set and that they must always be included in the error model. The terms of the 2nd-order radial and tangential distortion of the optics get very significant values (Table 2). The effect of higher-order polynomials was also studied but it was soon clear that they did not reduce the residual mean square error (r.m.s.e.) computed from the residuals of the displacement values.

Figures 6 and 7 show clearly that there is a periodic error in the direction of the drive system (sub-scan direction). Figure 7 indicates that this phenomenon remains from scan to scan. Image 1 differs from the other images in having a large number of gross errors. Its radiometric image quality is probably not fully stabilized, because the scanner was not tuned-up for long enough.

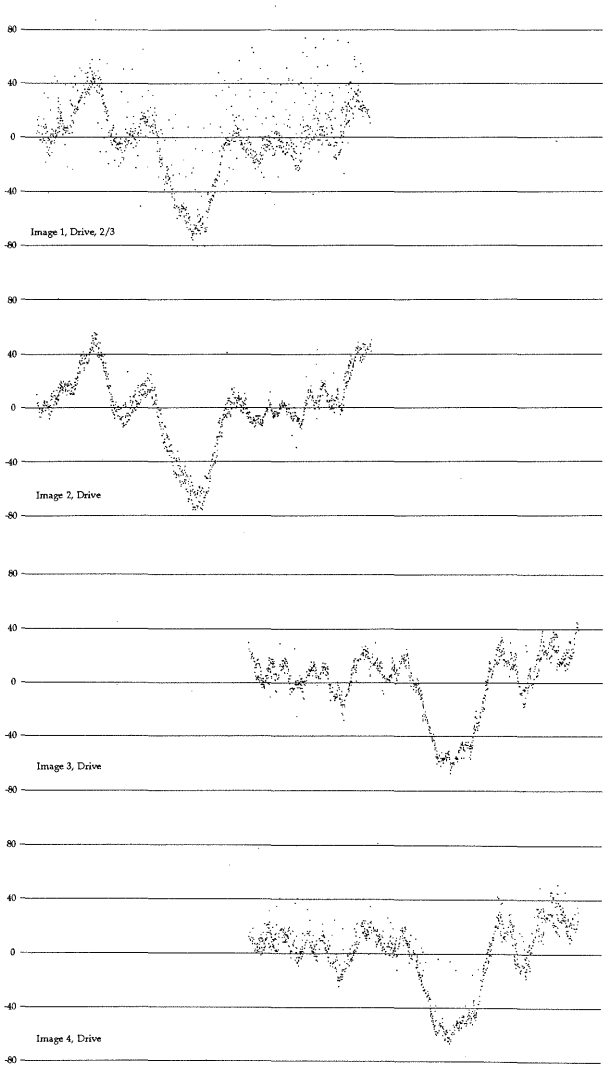

Figure 6. Systematic errors in the drive (sub-scan) direction. The residuals based on the basic model are plotted image-wise using a sub-scan projection .

Table 1. Statistics of the adjustment with the final error model. The area is restricted to a window of 10" (6000 lines x 6000 lines). Local corrections in the drive-direction are made with the bin interpolation, bin size = 50 lines. Gross errors (residual ≥ 30 μm) have been removed.

	Residual-mean-square-errors, μm			Final number of observations		Number of gross errors	
Image	Optics	Drive	Both	Optics	Drive	Optics	Drive
1	9.5	9.8	9.7	754	704	0	57
2	7.2	6.1	6.7	753	760	0	1
3	8.8	5.0	7.2	779	780	0	0
4	9.2	6.8	8.1	776	767	0	12
Totals	8.7	7.1	7.9				

Table 2. Effect of the polynomial parameters of the error model at the extreme points of the scanning area (10200 x 7032 pixels). The center point of the scanning area is assigned to be the origin. Consequently, all the parameters get zero-values in the center of the scanning area and maximums of the absolute values in the corners (where abs(x) = 5100 and abs(y) = 3516). The values refer to the same error model as in Table 1.

Parameter	Coefficient	Effect of the parameter (dx, dy) at the corners of the scanning area, μm
Main-scan direction (Optics)		
a_1	y	-26
a_2	y^2	-144
Sub-scan direction (Drive)		
b_1	x	-96
b_2	y	36
b_3	y^2	120

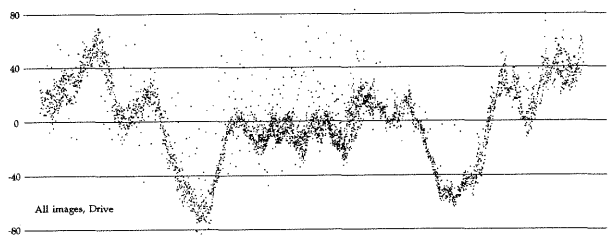

Figure 7. Systematic errors in the drive (sub-scan) direction. The residuals based on the basic model are plotted for all the images using a sub-scan projection.

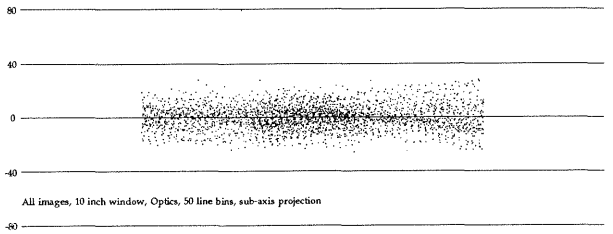

Figure 8. Systematic errors in the drive (sub-scan) direction. The residuals based on the basic model and local corrections with bin-interpolation (bin size: 50 lines) are plotted for all the images simultaneously in a window area of 10" using a sub-scan projection. All the gross errors (residual ≥ 30 μm) have been removed.

Figures 9, 10 and 11 display the errors in the direction of the optics (main-scan direction). It is seen that there are some systematic errors, particularly in Image 3, that the polynomial error model is unable to adopt. The deformation is caused by the tendency of the glass plate to be lifted 0.1 - 0.4mm at one end of the scan (bottom), thus immediately causing this kind of deformation. The ultimate reason is that the opposite end of the table "hangs in the air" without vertical support.

Figures 8 and 12 show the residuals based on the "final" adjustment, in which a window of 10" in the center of the scanning area is used. The local effects of the periodic errors have been compensated by using bins of 50 lines. Observations with residuals of $\geq 30\mu m$ have been removed as gross errors. Figure 12 shows that a main-axis dependent systematic error still remains in the optics.

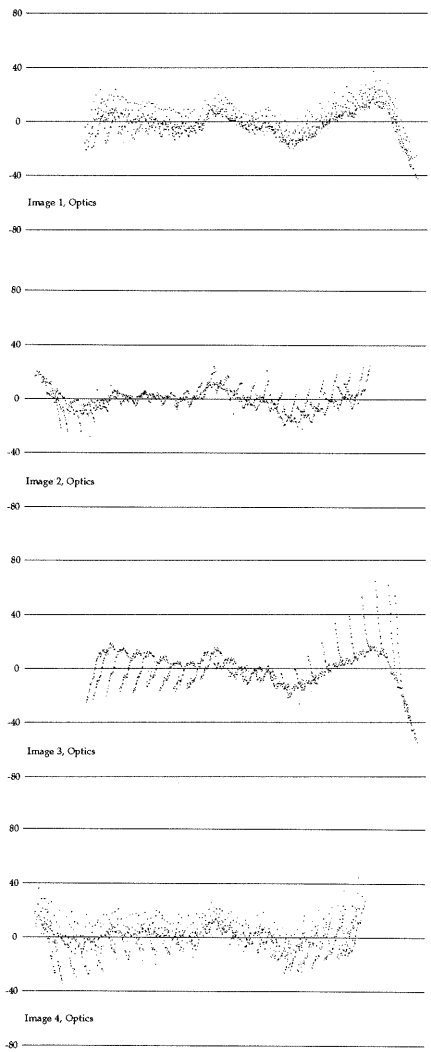

Figure 9. Systematic errors in the optics (main-scan) direction. The residuals based on the basic model are plotted image-wise using a main-scan projection.

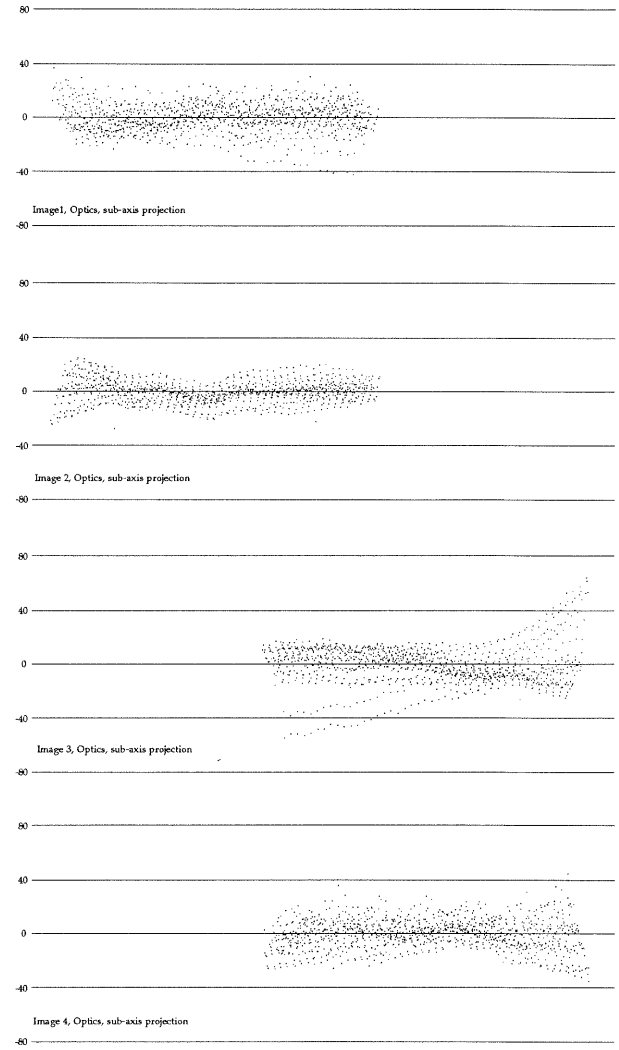

Figure 10. Systematic errors in the optics (main-scan) direction. The residuals based on the basic model are plotted image-wise using a sub-scan projection.

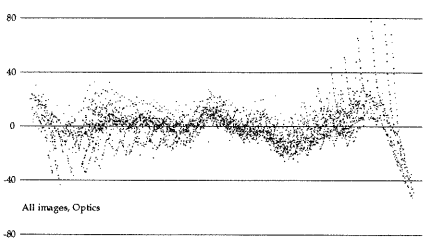

Figure 11. Systematic errors in the optics (main-scan) direction. The residuals based on the basic model are plotted for all the images simultaneously in a window area of 10" using a main-scan projection.

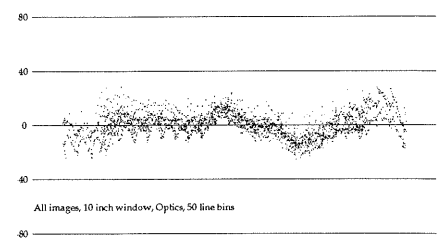

Figure 12. Systematic errors in the optics (main-scan) direction. The residuals based on the basic model are plotted for all the images simultaneously in a window area of 10" using a sub-scan projection.

Table 1 summarizes the statistics of this final adjustment. The r.m.s.e. value computed from all the observations is 7.9 μm, which is about 1/5 of the pixel size. There are no big variations in the r.m.s.e. values of the optics and drive system, although the values are slightly better for the drive system. This may be because the model did not take into account all the systematic errors of the optics.

3.6 Conclusions of the Calibration

The calibration procedure described above has convinced us that our original assumptions of the geometrical characteristics of the SHARP JX-600 scanner are to a great extent valid. The tests have shown that

- The use of photogrammetric grids and digital image processing methods is capable of producing observations with sub-pixel accuracy. The tests reported in this work show that the accuracy is on the order at least 1/5 of the pixel size of 42.3 μm. Additional tests have shown that even an accuracy of 1/10 of the pixel size can be achieved.

- The geometric deformations of the scanned imaged are very much as expected: the drive system causes a periodic systematic error in the sub-scan direction and the optical system causes strong systematic errors in main- and sub-scan directions, due to the 2nd order radial and tangential distortions. There is also a smaller periodic error in the main-scan direction that was not considered in our error model. In this respect the error model could be expanded.

- The stability or repeatability of the scanning results is rather good in terms of image geometry, at least within a short interval. The edges of the scanning area are problematic, owing to the table's insufficient guidance system. This should be improved to provide better vertical support to the front of the table.

- The magnitude of the geometric deformations is so great that they must be taken into account when the scanned images are used for photogrammetric purposes.

- With proper treatment of the systematic errors, the geometry of the scanned images can be controlled to give an accuracy level of at least 1/5 of the pixel size (r.m.s.e. value). This level satisfies the photogrammetric requirements very well.

- Only the center part of the scan area should be used for scanning aerial photographs 9" x 9" in size. Control of the geometrical distortions is best in the center area of the scanner.

4. PROPOSAL FOR CONTINUOUS CALIBRATION

The calibration procedure described above relies on the use of photogrammetric precision gitters which are scanned separately for calibration purposes. This approach is acceptable for periodic calibration. In every-day use the geometric quality of the scanned images should be monitored continuously. This can be done by scanning a geometrically precise test pattern or grid together with each image.

For calibration purposes it would be advantageous to have a grid completely covering the actual 9" x 9" scanning area. This is not feasible in practice as the grid pattern would be rather annoying on the scanned images. A grid surrounding the image frame would be more practicable as the frame could then be scanned with the image. The grid frame could be permanently engraved on the glass plate of the table. For scanning transparencies such as aerial photograph diapositives, a special scattering plate could be made of glass, having the grid frame engraved. This plate would also improve the flatness of the diapositive.

A calibration procedure similar to that described above should be made for each image separately. The horizontal parts (top and bottom) of the frame could be used to control the geometry in the main-scan direction, and the vertical parts (front and rear) in the sub-scan direction. Note that calibration would be fully automatic and thus no manual observation work is needed. The continuous calibration may also be regarded as a quality control and monitoring phase to confirm that the values of the parameters in the error model have not changed. If obvious changes are seen, their reason be pinpointed and the appropriate action taken.

5. IMAGE SHARPNESS

Image sharpness was studied briefly by scanning a non-transparent, black-and-white test chart. The chart was scanned in color-mode at three locations with respect to the main-scan direction: front, center, and rear. Figure 13 shows the results. In the center (b) 11 or 12.5 linepairs/mm are visible, in the rear (c) 9 or 10 and in the front (a) 8 or 9.

This test, although brief, confirms our general observation that image sharpness is best in the center of the scanning area, and that the front part of the image is somewhat less sharp than the rear. This asymmerty might be due to the optical system being out-of-focus. However, this could be corrected by proper adjustment. The slight unsharpness that remains at the edges is typical of optics-based imaging systems.

Some experiments were carried out to compare color and gray-scale scanning modes. The results for the color mode were at least as good as those for the gray-scale mode. In some cases, image resolution (linepairs/mm) in the sub-scan direction was slightly better in the color-mode.

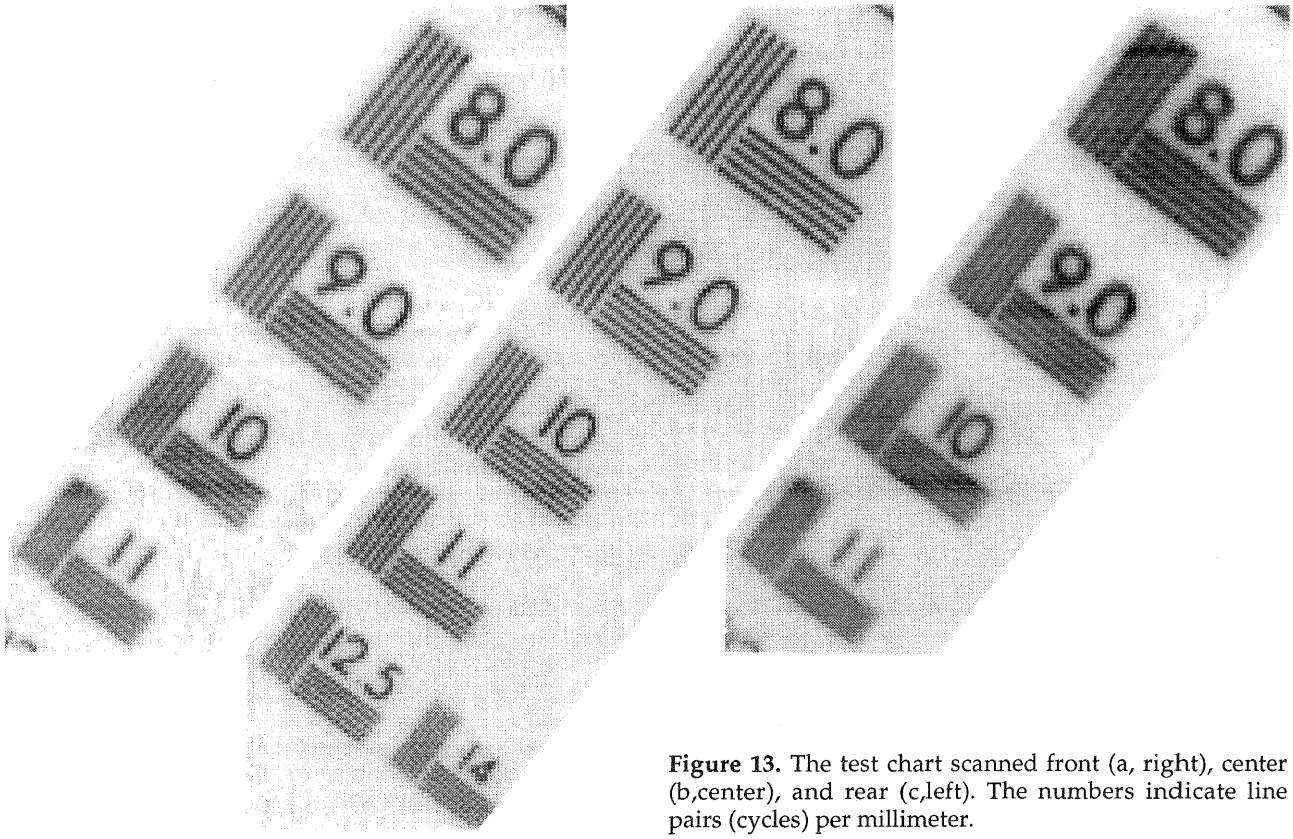

Figure 13. The test chart scanned front (a, right), center (b,center), and rear (c,left). The numbers indicate line pairs (cycles) per millimeter.

6. CONCLUSIONS AND RECOMMENDATIONS

Regarding the use of the Sharp JX-600 scanner for photogrammetric purposes, there are considerable geometrical deformations in the scanned images. The stability of the scanner, altough rather good, it could be further improved by modifying the guidance system to eliminate vertical movements of the table. The geometry of the scanned images can be controlled with an accuracy of 1/5 of the pixel size, or 8 μm, if proper scanning procedures and calibration methods are applied. The center part of the scanning area should be used for scanning as the geometric deformations can be controlled most reliably there. The center part also produces the sharpest imaging. A continuous calibration method based on the use of special grid frames at the edges of the image is proposed as the most robust method for controlling geometric quality.

The calibration method and related computer programs developed in this study have also general applicability and could be used to calibrate image scanners with resembling opto-mechanical structure.

With proper treatment of the systematic errors, the geometry of the scanned images can controlled to yield an accuracy level of at least 1/5 of the pixel size (r.m.s.e. value). This level is satisfactory for photogrammetric purposes. A prerequisite is that the values of the error model parameters are used for the corrections needed at all the photogrammetric phases, e.g. determination of the orientation parameters and digital rectification of the images.